

1 Article

2 **Electrochemical Activity of Lignin Based Composite**  
 3 **Membranes.**

4 **Marya Baloch**<sup>1</sup>, **Mikel Alberro Astarbe**<sup>2</sup> and **Jalel Labidi**<sup>1,\*</sup>

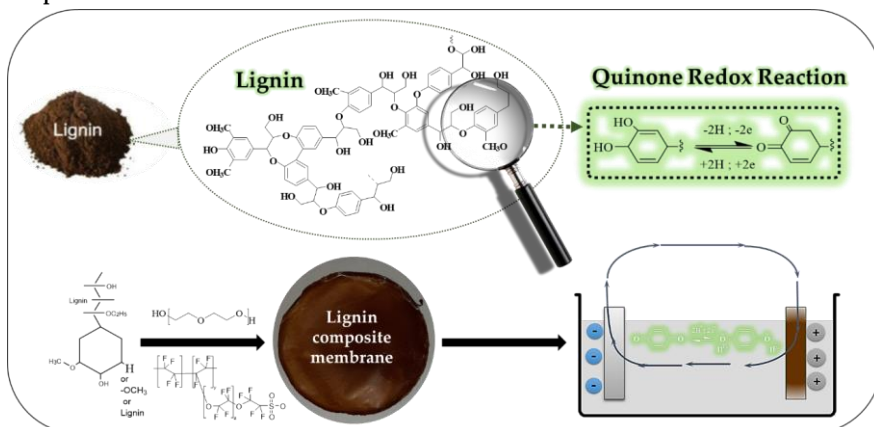
5 <sup>1</sup> Department of Chemical and Environmental Engineering, Faculty of Engineering, Gipuzkoa,  
 6 Donostia-San Sebastian; marya.baloch@ehu.eus, jalel.labidi@ehu.eus

7 <sup>2</sup> Department of Electronic Technology, Faculty of Engineering, University of the Basque Country  
 8 (UPV/EHU), Plaza Europa 1, 20018, San Sebastian, Spain; mikel.alberro@ehu.eus

9 \* Correspondence: jalel.labidi@ehu.eus; Tel.: +34-943-01-7178

10 Received: date; Accepted: date; Published: date

11 **Graphical Abstract:**



12

13 **Key Highlights:**

- 14 ○ Successful fabrication of lignin polymeric composite membrane electrodes via facile and low-cost
- 15 method.
- 16 ○ Exploration of lignin’s quinone functionality and its electrochemical activity.
- 17 ○ Achievement of enhanced functionality and improved conductivity of lignin by mixture
- 18 composites.

19 **Abstract:** Our society’s most pressing challenges like high CO<sub>2</sub> emission and the constant battle  
 20 against energy poverty needs a clean and easier solution to store and utilize the renewable energy  
 21 resources. However, recent electrochemical components are expensive and harmful for the  
 22 environment, which restricts their widespread deployment. This study proposes an easy method to  
 23 synthesize and fabricate composite membranes with abundantly found biomass lignin polymer to  
 24 replace conventional costly and toxic electrode materials. Easier manipulation of lignin within the  
 25 polymeric matrix could provide the improved composite to enhance its electrochemical activity. Our  
 26 major focus is to activate, the quinone moiety via oxidation in the polymeric mixture using a strong  
 27 ionic acid. The physico-chemical and electrochemical characterizations of two different lignins with

28 different polymeric mixture compositions have been carried out to confirm that the redox properties  
29 of pure unmodified lignin could be achieved via intrinsic mutual sharing of the structural properties  
30 and intercross linkage leading to improved integrity and redox activity/conductivity.

31 **Keywords:** Batteries, Lignin, Inexpensive, Environmentally Friendly, Quinone, Redox Activity.  
32

---

### 33 1. Introduction

34 Electric energy storage systems are widely demanded by various sectors both for their great  
35 versatility and advantages as environmentally sustainable alternatives such as storage of energy from  
36 renewable resources.[1,2] With growing population, the CO<sub>2</sub> emissions from internal combustion  
37 engines are increasing, with a terrible effect both on personal health and the environment. From  
38 electrochemical energy storage, batteries are the systems with the highest storage capacity, due to  
39 their high energy density.[3–5] Although, batteries are efficient, convenient, reliable and easy to use,  
40 their useful life and autonomy are limited, in addition to their doubtful sustainability in terms of  
41 materials, since the materials used (both metals and non-metals) can generate various polluting  
42 constituents during the process.[6] Therefore, the practicality of these inorganic materials is limited  
43 by various factors such as scarcity, high cost, toxicity and difficulty of processing procedures. It is  
44 essential to find a replacement of these materials with the materials that are abundant and sustainable  
45 i.e. organic polymers.

46 The redox polymers have gained popularity as a replacement to harmful battery components due to  
47 their non-toxic nature and enhanced electrical properties such as poly(3,4-ethylenedioxyphene)  
48 (PEDOT),[7] polyaniline (PANI),[8] polythiophene (PTh),[9] polypyrrol (PPy),[10] polyacetylene  
49 (PA),[11] polycarbazol (PC) [12]. Unlike inorganic materials, they show properties such as low  
50 viscosity, low thermal conductivity, easy processing in versatile shapes, and adjustable molecular  
51 structures.[13] However, conversion of polymeric compounds into carbon is widely used, due to their  
52 diversity in shapes and structures i.e. carbon fibres, activated carbon, and graphene, etc.[14] These  
53 materials confer great benefits, such as mechanical improvements or increased conductivity.[15]  
54 Furthermore, they can be derived from natural sources such as wood,[16] which is mainly  
55 composed of cellulose, hemicellulose and lignin. [17]

56 Lignin is a highly complex aromatic biopolymer, which is usually found in larger quantities around  
57 the world, typically used as a source of fuel or an additive[18,19] in bio-mass material applications.  
58 Implementation of lignin within applications with higher added value has been extensively studied  
59 for decades, however, the field of energy storage systems can be added as a novel application already  
60 holding numerous investigations in various topics, though, lignin as bulk so far only have been used  
61 for generating heat energy.[20] Due to its insulating nature, improvement in its electrochemical  
62 properties/ redox activity could be challenging, nonetheless, lignin offers an enriched vital functional  
63 groups like hydroxyl (-OH), methoxy (OCH<sub>3</sub>), aldehyde (CHO) and carbonyl (C=O) that supports  
64 easy processing in synthetic monomers and polymers. The highly rich aromatic structure of lignin  
65 allows fabrication of low-cost, activated and well-ordered carbons in distinctive shapes and  
66 forms.[21–24] Lignin has already been exploited in different battery systems as binder,[25,26]  
67 electrolyte[27] and as an additive,[28,29].

68 It has been established that modified and treated lignin could affect positively towards discharge  
69 performance of the battery.[30,31] In the meantime, the study of the impacts of different lignin  
70 components and the charge storage capacity of lignin have shown the redox activity (combined  
71 faradaic/non-faradaic charge storage) proving that by adding non-modified lignin, the capacity of the

72 mixture could increase due to electrical double layer (EDL) charge storage that is usually dependent  
73 of the surface area. Hence, the final composite product can provide charge storage capacity  
74 depending on the mixing ratio and surface area. However, the highest capacity could be achieved via  
75 exposure of lignin functionalities towards electrolyte, homogeneity and high surface area, even  
76 though with the unmodified commercial one.[32–39] In order to allow faster transfer of charge  
77 storage, lignin needs suitable alterations, whether it is by chemical or physical inter-cross linking,  
78 thereby, enhancing electronic conductivity and helping with the electroactive redox activity[40,41].

79 The main goal of this study is to achieve low cost and easy-processed lignin based composite  
80 membranes with improved redox activity. The commercial unmodified organosolv lignin has been  
81 used, due to its higher relative amount of phenolic hydroxyl functional groups, although, freshly  
82 extracted kraft lignin has also been used to observe the effect of sulphur groups over redox chemical  
83 reaction of. Trials of different ratios and optimization has been carried out, the mixture was further  
84 stabilise with the help of non-ionic plasticizer polymer such as polyethylene oxide (PEO), which also  
85 help in providing extra –OH groups within the mixture. Mild reaction conditions and simple mixing  
86 techniques have been employed to prepare the blends of lignin to emit multiple modification reaction  
87 steps in favour of affordable and ecological approach. A strong acidic nature polymer, Nafion®  
88 has been considered for the easy cleavage of covalent bonds to enhance the possibility of inter-cross  
89 linkage that provides the adequate charge for the ionic transfer via chemical/ physical interaction of  
90 lignin and assuming that within the process of constant stripping/plating process, these membranes  
91 displays the promising longer stripping/plating cycle life. To our knowledge, this is the first attempt  
92 to prepare lignin composite polymeric matrix with PEO adding a strong ionic acid i.e. Nafion® with  
93 mild conditions, the aim is to coerce potential lignin electrochemical redox activity by activating its  
94 quinone functionality. There have been several studies about the activation of methoxy group  
95 resulting quinone species via oxidation of guaiacyl (G) and syringyl (S) aromatic alcohol units.[42–  
96 44] Upon forming the quinone species, charge transfer process initiates within the surface of electrode  
97 and electrolyte. On that basis, we have considered the quinone as a major functionality of lignin  
98 interacting during the electrochemistry of the composite membranes when in electrolytic solutions  
99 under certain conditions. Nevertheless, NF, itself provide enough charge for the ionic transfer via  
100 chemical or physical interaction with lignin. The lignin composites were ~~characterised~~characterized  
101 via physico-chemical and electrochemical measurements to ~~analyse~~analyze the synergic arrangement  
102 of the composite.

Formatted: Font: Not Bold

Formatted: Font: Not Bold

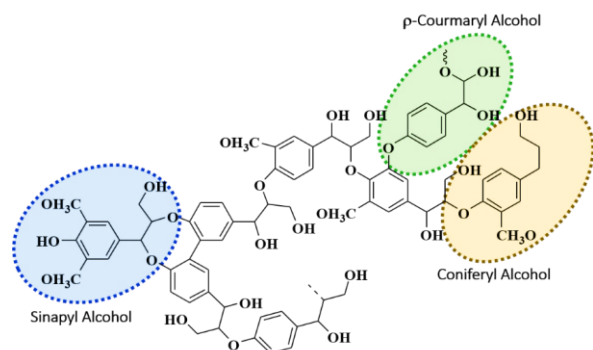
Formatted: Font: Not Bold

## 103 2. Materials and Methods

104 Organosolv commercial lignin was purchased from Chemical Point UG (Oberhaching, Germany) and  
105 Nafion® Perfluorinated resin powder from Ion Power Inc. (The Chemours Company). Polyethylene  
106 oxide (PEO: M.W. 100,000), Dimethyl sulfoxide (DMSO), Ethanol (EtOH), and Sulfuric acid (H<sub>2</sub>SO<sub>4</sub>)  
107 were purchased from Sigma-Aldrich. Kraft lignin was freshly extracted from black liquor received  
108 by a local paper industry (Papeleria Guipuzcoana de Zicuñaga) of eucalyptus source.

### 109 2.1. Lignin:

110 Two types of lignins have been used in experimentation, commercially available organosolv lignin  
111 (Softwood) and freshly extracted kraft lignin from black liquor of local paper pulp industry  
112 (Hardwood). The general structure and major units of lignin have been shown in figure 1. Lignin  
113 have three major composing aromatic alcohol units, sinapyl, coniferyl, and p-coumaryl (Figure 1),  
114 the difference between these alcohols is linkage of methoxy group on the phenol structure. These  
115 alcohol later form the monolignols of lignin i.e. syringyl (S), guaiacyl (G) and p -hydroxyphenyl (H).  
116 [45–49]



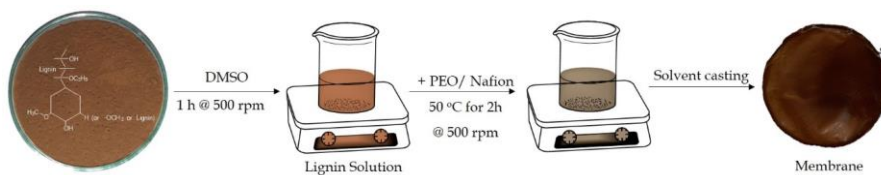
117 **Figure.1:** Chemical structure representation of lignin showing its major aromatic alcohol units.  
 118  
 119 The lignins have been thoroughly characterized within our research group "BioRP", the ratios and  
 120 values of H, G, S, and ratio of S/G (Table. 1) have been calculated via pyrolysis of mentioned lignins.

Type	Source	Origin	Ratios			
			S	G	H	S/G
Organosolv	Commercial	Softwood	15.57	42.77	9.28	0.36
Kraft	Liquor paper industry	Hardwood	64.88	32.20	1.42	2.01

121  
 122 **Table 1:** Source, Origin and monolignols ratios of used lignins.

### 123 2.2. Preparation of Lignin based composite membranes

124 The composite membranes were prepared by using DMSO solvent technique. Oven dried lignin was  
 125 dissolved in different quantities in a closed vial (Table S1, Figure 2). PEO and Nafion® polymer  
 126 solution was prepared in acetonitrile under the vigorous stirring, until the powder was completely  
 127 dissolved. The mixture solution was transferred into the lignin solution, the mixture was left at the  
 128 reaction temperature of 50 °C with continuous stirring for 2 h. The concentration of mixture solution  
 129 was maintained at 5 wt. %. OLPO, OLNf, and OL/KLPONF composite membranes were obtained by  
 130 solvent casting the homogeneous lignin-polymer mixture in Teflon dish and dried at 40 °C.



131  
 132 **Figure.2:** Illustration of the preparation process of Lignin based composite membranes.

133 The obtained dried membranes, light brown to darker brown in colour were punched out into 20mm  
 134 discs to be used as working electrodes in electrochemical characterizations. The mixture containing  
 135 higher percentage of lignin resulted into a thick gel to hard rock pieces, which were difficult to  
 136 manage and analyze.

### 137 2.3. Characterization

138 The water uptake (WU), swelling ratio (SR) and gel content percentage (GC) test were carried out  
 139 with oven dried composite membranes (~2.49 × 1.5 × 0.075) in de-ionised (DI) water at room  
 140 temperature. After 24 hours the membranes were collected and measured to calculate the values of  
 141 WU, SR and GC percentage equation S1, S2 and S3 have been used, respectively (Detailed procedure  
 142 in supplementary information).

143 Fourier transform Infrared spectra (FTIR) Spectroscopy measurements were attained on a  
 144 PerkinElmer Spectrum Two FT-IR Spectrometer equipped with Universal Attenuated Total  
 145 Reflectance (UATR). All measurements were done ranging from 400 to 4000  $\text{cm}^{-1}$  at room temperature  
 146 with 64 average scans. Differential scanning calorimetry (DSC) measurements were carried out on  
 147 DSC822e (Mettler Toledo) in the range of room temperature to 500°C under  $\text{N}_2$  atmosphere with the  
 148 heating rate of 10°C  $\text{min}^{-1}$ .

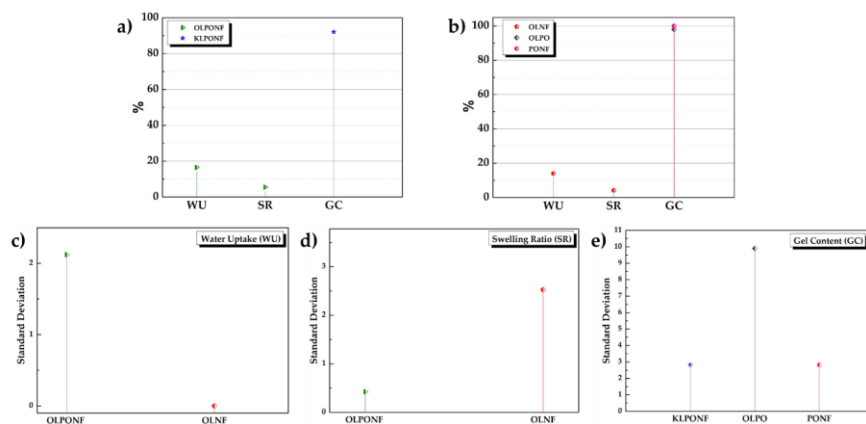
149 Electrochemical measurements were carried out at room temperature with mild flow of  $\text{N}_2$  gas using  
 150 Solatron Multipotentiostat 1480 and Solatron mobrey SI 1260 (Impedance-Gain phase analyser) in a  
 151 conventional three-electrode electrochemical cell with a wide platinum foil as a counter electrode and  
 152 an Ag/AgCl reference electrode. The electrochemical activity of the composite materials was  
 153 evaluated in aqueous solutions of 1 M  $\text{H}_2\text{SO}_4$ . CV measurements were performed at different scan  
 154 rate of 5, 10, 20, 30, and 50  $\text{mVs}^{-1}$  in the range of -1V to 1V. EIS spectra were scanned within a  
 155 frequency range of 0.01Hz to 100000 Hz with AC amplitude of 10 mV at room temperature.

156 Error of the repeated data of WU, SR, GC and EIS have been calculated by statistical calculation as a  
 157 function of standard deviations (SD) and ratio of variances to ensure the behavioural changes and  
 158 variability within different composites.

### 159 3. Results

#### 160 3.1. Water Uptake (WU), Swelling Ratio (SR) and Gel Content (GC) % tests

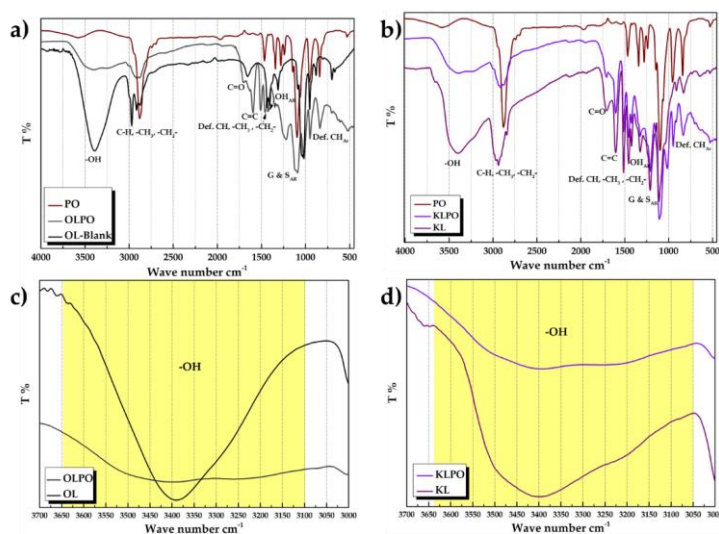
161 The membranes were analyzed by water uptake and swelling ratio test, due to presence of polymers  
 162 in the lignin composite with relatively high hygroscopic ratio. The figure 3 shows the average WU,  
 163 SR and GC % of different membranes.



164  
 165 **Figure 3: (a-b) Representation of the percentage rate of WU, SR and GC contents in different**  
 166 **composite membranes, (c-e) Error statistical analysis via standard deviations (SD) with respect to**  
 167 **their mean values.**

168 The water uptake capacity of lignin/ polymer composite membranes showed lower rehydration  
 169 ratios, probably due to the pore generation/swelling owing to their lower thickness. The thickness  
 170 can be a crucial factor for the pore sizes and porosity of material. PONT, OLPO and KLPONF  
 171 exhibited Gel content of 100, 98 and 92%, probably due to the sulphur group in kraft lignin and  
 172 hygroscopic nature of the PEO. Though, it might lead to the poor mechanical properties and high-

173 water ions permeability. However, addition of OL lignin in PONF mixture increases the integrity of  
 174 the membrane, perhaps owing to the successful crosslinking, providing an advantage of stronger  
 175 mechanical properties. The error calculated via statistical analysis of the repeated samples during  
 176 WU and SR tests shows that the behavior of each membrane is quite different depending on the  
 177 composite mixture that plays an important role in their structural integrity, for example, in the case  
 178 of WU and SR, OL PONF and OLNF shows the difference of ~2-2.5 points, respectively. That could  
 179 accord with the hygroscopic nature of PEO in OL PONF membrane to help absorb higher amount of  
 180 water than OLNF. However, the physico-chemical intercross linkage between PEO and lignin in the  
 181 presence of NF provides a firm wholeness to avoid membrane dissolution, which could be confirmed  
 182 by OLPO membrane's total disintegration. Comparing the lignins, in the case of KLPONF, the  
 183 membrane totally disintegrated and thus the highest GC % and SD have been calculated, as  
 184 mentioned, structural integrity is achieved via composite mixtures is totally depend on their nature,  
 185 which give a clue that this might be due to correlation of sulphur group in KL with sulphonic groups  
 186 ( $-\text{SO}_3\text{H}$ ) of NF. The thorough studies are needed to understand this phenomena.



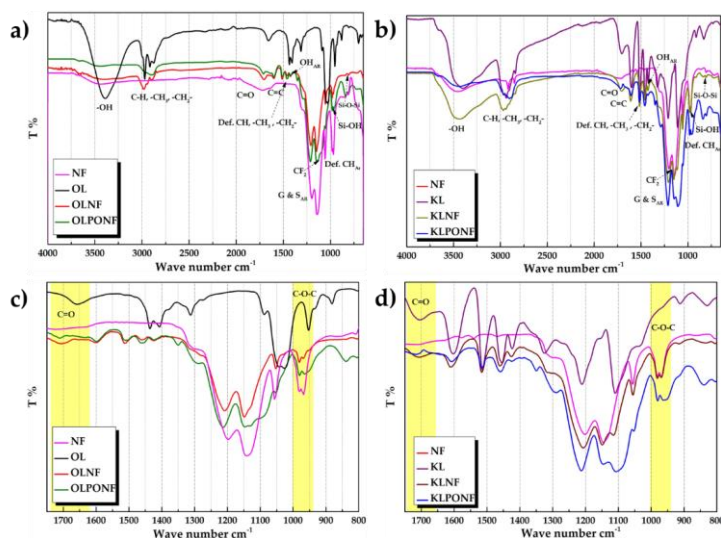
187

188 **Figure 4:** FTIR spectra a) Organosolv lignin-PEO (OLPO) composite in comparison to PEO (PO)  
 189 and blank organosolv lignin (OL) b) comparison of OLPO and OL to demonstrate shift in peak in  
 190 the range of  $3000\text{--}4000\text{cm}^{-1}$  c) Kraft lignin-PEO (KLPO) composite in comparison to PEO (PO) and  
 191 blank kraft lignin (KL) d) comparison of KLPO and KL to demonstrate shift in peak in the range  
 192 of  $3000\text{--}4000\text{cm}^{-1}$ .

### 193 3.2. Fourier Transform Infra-Red (FTIR) Spectroscopy and Differential Scanning Calorimetry 194 (DSC)

195 FTIR spectra validates the incorporation of polymer components with lignin functionality and  
 196 confirms the physico-chemical crosslinking. Figure. 4 displays FTIR spectra of the pure lignin  
 197 (OL/KL), PEO (PO) and lignin-PEO mixture (KL/OLPO, 80:20) mixture. OLPO and KLPO mixture  
 198 shows comparable peaks as of non-modified lignin (OL/KL) with slight shift in the wavenumber.  
 199 Lignin usually shows OH stretching vibration in a shape of broaden peak between 3045 and 3562

200  $\text{cm}^{-1}$ , basically due to the presence of alcoholic and phenolic hydroxyl groups, whereas the  
 201 characteristic peaks of PEO appears around  $3585 \text{ cm}^{-1}$  and  $1096 \text{ cm}^{-1}$ . In the composite mixture, a  
 202 broad peak with slight shoulder corresponding to OH stretching appears between  $\sim 3673\text{-}3057$   
 203 (OLPO) and  $3714\text{-}3031 \text{ cm}^{-1}$  (KLPO).[50] Alkyl group ( $-\text{CH}_2$ ,  $-\text{CH}_3$ ,  $-\text{CH}_2-$ ) has an intense band at  $\sim 2939$   
 204  $\text{cm}^{-1}$  and at  $2844 \text{ cm}^{-1}$ , and aromatic  $\text{C}=\text{C}$  stretching at  $\sim 1599$  and  $1504 \text{ cm}^{-1}$ . A new band at  $1594 \text{ cm}^{-1}$   
 205 appeared i.e. possibly corresponding to the stretching of aromatic ring of lignin, peaks of  $-\text{OH}$   
 206 bending vibrations of the aromatic ring appears at  $1459$ ,  $1424$ ,  $1351$  and  $1328 \text{ cm}^{-1}$  and  $\text{C}-\text{O}-\text{C}$   
 207 stretching vibration at  $1210$ ,  $1108$  and  $1031 \text{ cm}^{-1}$ . In some literature, the particular peaks at  $1328 \text{ cm}^{-1}$ ,  
 208  $1210 \text{ cm}^{-1}$ , and  $1108 \text{ cm}^{-1}$  were assigned to the vibrations of syringyl rings and guaiacyl rings. The  
 209 band at  $834 \text{ cm}^{-1}$  in KL represents the deformation vibrations of  $\text{C}-\text{H}$  bonds in the aromatic rings.,  
 210 which usually corresponds to the aromatic  $-\text{OH}$  stretching, whereas aliphatic  $-\text{CH}$  stretching appears  
 211 at  $\sim 2879 \text{ cm}^{-1}$ ,  $-\text{CH}$  bending at  $1466 \text{ cm}^{-1}$  and  $1341 \text{ cm}^{-1}$ .  $\text{C}-\text{O}-\text{H}$  stretching shows a peak at  $1279$   
 212  $\text{cm}^{-1}$ . [51]

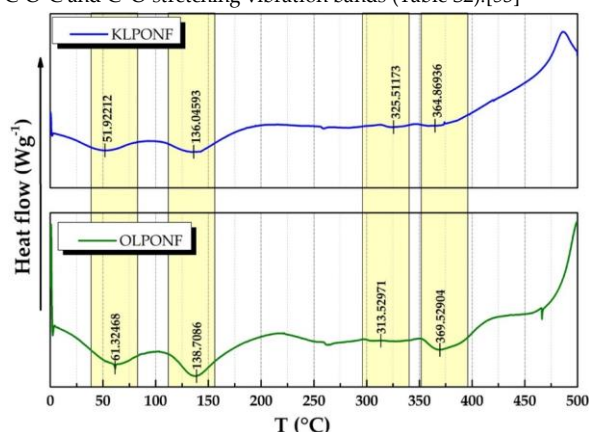


213  
 214 **Figure 5:** FTIR spectra a) OLPONF and OLNf composite in comparison to NF and OL b)  
 215 comparison of  $\text{C}-\text{O}-\text{R}$  and  $\text{C}=\text{O}$  groups to demonstrate shift in peak. c) KLPONF and KLNf  
 216 composite in comparison to NF and blank kraft lignin d) comparison of  $\text{C}-\text{O}-\text{R}$  and  $\text{C}=\text{O}$  groups to  
 217 demonstrate shift in peak.

218 The shoulder of the broad peak at  $3226 \text{ cm}^{-1}$  could be due to the intermolecular  $-\text{H}$  bonds of aliphatic  
 219 hydroxyl groups. The peak at  $3404 \text{ cm}^{-1}$  corresponds to intermolecular dimer OH peak.  
 220 Intermolecular bonded OH peak at  $3236 \text{ cm}^{-1}$  is a shoulder appearing in OLPO and KLPO, even  
 221 though KL shows the slight shoulder itself, however in the case of the mixture the low intensity of  
 222 the band could prove the formation of Intermolecular hydrogen bonding confirming cross-linkage of  
 223 lignin with PEO.[52]

224 FTIR spectra (Figure 5) of OLPONF and KLPONF has been compared with the NF, OL and KL  
 225 spectra, mostly the peak resembles the mixture of lignin and Nafion®, however, the peaks of PEO  
 226 seems to be overlapped by the OLNf mixture. In the spectra, the peaks which seems to have a

227 shoulder in the region of  $\sim 980.64\text{ cm}^{-1}$  in OL/KLNF and OL/KLPONF are probably corresponding to  
 228 the C-O-C group of Nafion® that usually appears slightly shifted ( $981.21\text{ cm}^{-1}$ ) in pure NF. The peak  
 229 at  $\sim 960\text{ cm}^{-1}$  corresponds to Si-OH, Si-O-Si at  $804\text{ cm}^{-1}$  instead of  $809\text{ cm}^{-1}$ , and  $\text{CF}_2$  within the region of  
 230  $1100\text{--}1200\text{ cm}^{-1}$ . C=O peak has shifted from  $1656\text{ cm}^{-1}$  to  $1712\text{ cm}^{-1}$ , which in OL/KLNF also appears  
 231 around same shift. The changing behaviour and impact of NF on the functionality of lignin is still yet  
 232 to be discovered in depth, however, the possible interconnection could be proven on the bases of  
 233 slight shifting of C-O-C and C=O stretching vibration bands (Table S2).[53]

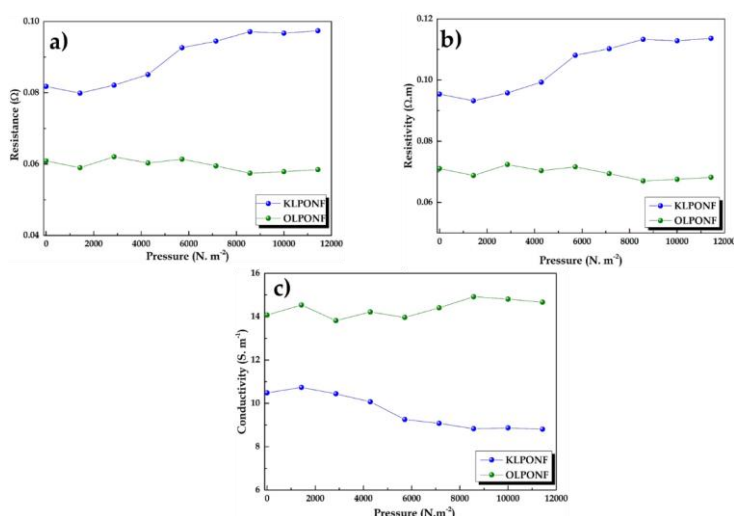


234  
 235 **Figure 6: Differential scanning calorimetry (DSC) curves of lignin based composite membranes.**  
 236 Differential scanning calorimetry (DSC) measurements of the lignin based composite membranes  
 237 was performed to study the thermal changes within composites blends (Figure 6), which shows the  
 238 characteristic peaks of PEO, lignin, and Nafion®. The endothermic curve following by exothermic  
 239 peaks within the regions of  $35\text{--}150^\circ\text{C}$  and  $300\text{--}400^\circ\text{C}$ , usually, corresponds to fusion or melting and  
 240 crystallization, respectively. However, KLPONF shows intense peaks, possibly due to the sulphur  
 241 groups of kraft lignin or sulfonic acid ( $-\text{SO}_3\text{H}$ ) groups of Nafion®. These results will need further  
 242 confirmation by thermogravimetric analysis (TGA) studies.

### 243 3.3. Conductivity measurements

244 The pressure dependent resistance and conductivity plot as a function of resistivity of OLPONF, and  
 245 KLPONF are shown in figure 7a. The resistance of KLPONF membrane seems to considerably alter  
 246 depending on the pressure applied, however, OLPONF membrane shows more or less constant  
 247 plateau, which could be refer to its better mechanical properties as demonstrated in wetting test. The  
 248 conductivity of these membranes has been calculated within the range of  $10\text{--}14\text{ S m}^{-1}$ , which could be  
 249 sufficient considering the fact that lignin is well-thought-out as an insulating material. The  
 250 conductivity measurements are yet to be confirm by the help of EIS techniques.





251  
 252 **Figure 7a: The variations of KLPONF and OLPONF membranes in terms of a) Resistance, b)**  
 253 **Resistivity and c) Conductivity with reference to applied pressure.**

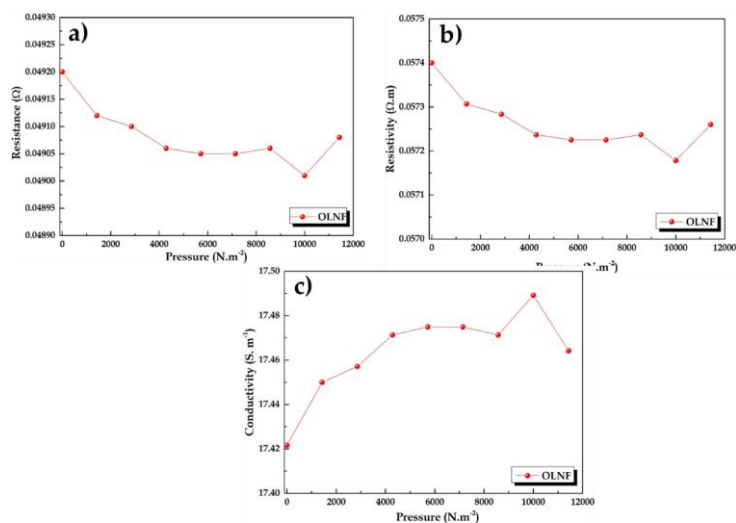
254 In order to test the theory of increased conductivity of lignin via composite mixture within ionically  
 255 rich polymer matrix, the tests have been repeated with the membrane only with lignin and nafion®  
 256 (OLNF) (Figure. 7b). The attempts to record the resistance and conductivity of the KLNf mixture  
 257 membrane was unsuccessful due to brittleness of membrane, which broke upon applying pressure,  
 258 however, sometimes we achieved a gel type membrane that usually stick to the surface of Cu  
 259 electrodes and made it quite difficult to follow the calculation procedure.

260 The OLNf membrane shows improved conductivity than OLPONF i.e. ~17-18 Sm<sup>-1</sup>. Although, this  
 261 humble change in conductivity open up the vast door for the diverse possibilities to caper and tune  
 262 it as required.

263 An attempt to measure the conductivity in a liquid phase (organic solvent) was done, in order to have  
 264 an assurance of the direct influence of Nafion® on the conductivity. It seems to decrease up to ~10<sup>-4</sup>,  
 265 owing to the fact that Nafion®'s hydrophilic sulfonate groups could improve the solubility of  
 266 quinone in water resulting ionization and production of aromatic anion. However, in the case of  
 267 organic solvents the ionization - of quinone was restricted, which affected the conductivity. Usually,  
 268 in the case of liquids, the conductivity shown within a mixture solution is proportional to its ion  
 269 concentration.

Solid	Liquid
$1.742 \times 10^{-1} \text{ S.cm}^{-2}$	$1.79 \times 10^{-4} \text{ S.cm}^{-2}$

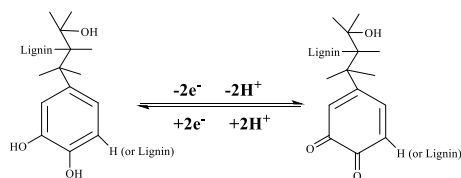
270  
 271  
 272  
 273 To explain the loss of hydrophilic groups during the solution submersion, the conductivity has been  
 274 noted after the wetting test, the OLPONF membranes were chosen on the basis of their higher  
 275 mechanical intactness, the resistance and resistivity surprisingly increased after submersion, and  
 276 there was a drop in conductivity that remain constant after applying pressure within the range of  
 277 1000-12000 Nm<sup>-2</sup>(Figure. S2).



278  
279 **Figure 7b: The variations of OLNf membranes in terms of a) Resistance, b) Resistivity and c)**  
280 **Conductivity with reference to applied pressure.**

### 281 3.4. Cyclic Voltammetry (CV) measurements

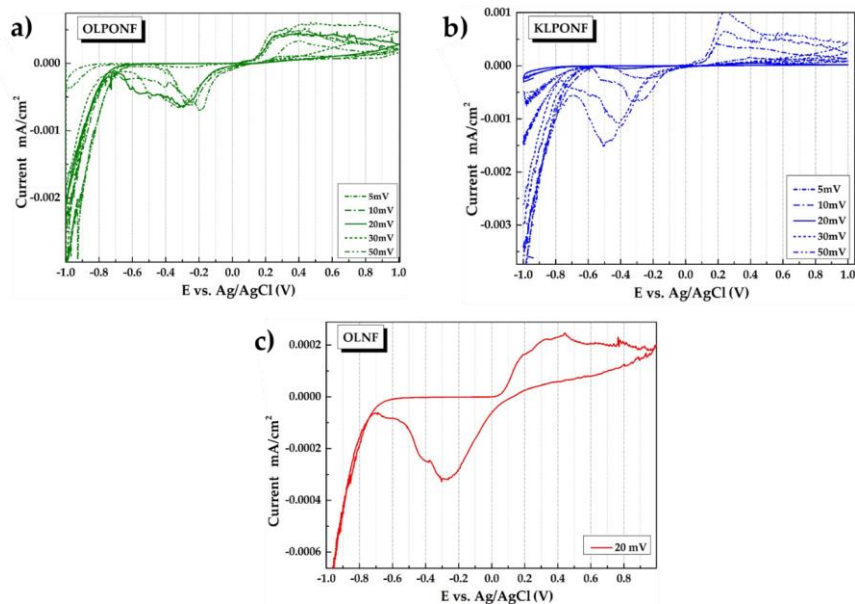
282 Figure 8 shows the cyclic voltammetry (CV) profiles performed in the window of -1 to 1V potential  
283 range for the OLPONf and KLPONf as WE at different scanning rates to follow the redox activity  
284 corresponding to the quinone functionality of lignin (OL/KL) composite mixture. Meanwhile, the  
285 profiles for OLNf electrodes was measured at the scan rate of 20 mVs<sup>-1</sup> for the comparison. Usually,  
286 the quinone moiety shows a sharp oxidation peak at ~0.6 V and an obvious reduction peak at ~0.4  
287 V, however, the oxidation and reduction peak appears to shift to ~0.37-4V and ~0.3-0.6V vs. Ag/AgCl  
288 (Sat. KCl), respectively, possibly demonstrating the coordination interactions of ether oxygen of PEO  
289 and Nafion®'s carbonyl oxygen atoms of lignin, it might also be the hindrance due to SO<sub>3</sub>H (sulfonic  
290 acid) group of Nafion®. The reversible faradic quinone/hydroquinone conversion reaction has been  
291 demonstrated in the schematic 1, where quinone functionality lose and gain 2 electrons/protons  
292 during the discharge and charge process.



293  
294 **Schematic. 1: Redox activity of quinone/hydroquinone functionalities during charge-discharge**  
295 **process.**

296 The sweep of different potential rate has been performed from 5-100 mVs<sup>-1</sup>, however there wasn't  
297 any significant changes in the current rate, that could be due to the possibility of constant ion-  
298 adsorption dependent redox processes, this constant behaviour could be explained by the fact that  
299 the acidic electrolyte has been changed after each experiment, which could provide the constant ionic

300 mobility. The constant current profile could also be due to constant ratio of lignin in the sample  
 301 electrodes.

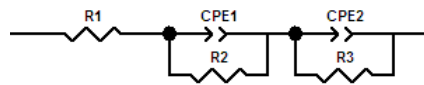


302  
 303 **Figure 8:** Shows the four cyclic voltammetry (CV) profiles of the OLPO, OLNE, OLPONF and  
 304 KLPONF electrodes performed in the window of -1V to 1V potential range at the scan rate of 20  
 305 mVs<sup>-1</sup>.

306 The voltammogram of the samples with higher concentrations i.e. thicker gel like lignin composite  
 307 shows very little redox activity, probably due to the insulating nature of lignin and the disintegration  
 308 within the electrolytic solution, however, the low amount of ionic polymer wouldn't have any  
 309 significant contribution to the electron storage.

### 310 3.5. Electrochemical Impedance Spectroscopy (EIS)

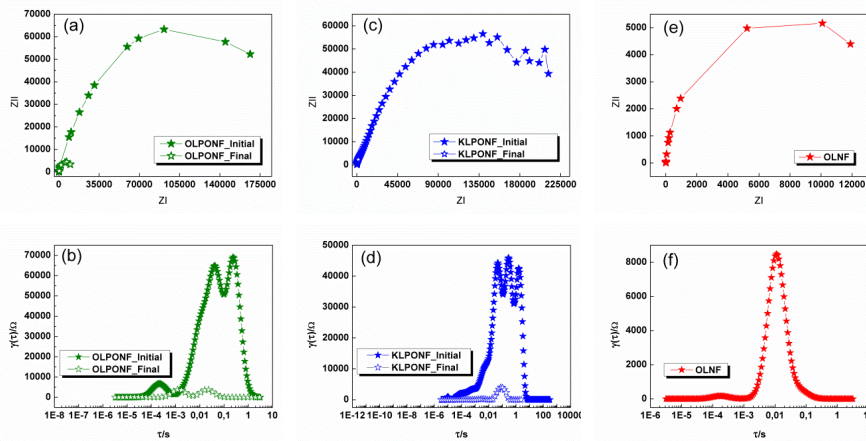
311 To further interpret the electrochemical performance, galvanostatic charging and discharging of the  
 312 lignin composite mixtures was conducted. Though, the active mass loading of lignin has been  
 313 maintained to 4 mg/mL. The charge–discharge 10 cycle curves at the current density of 100 mA.cm<sup>-2</sup>  
 314 between -1 and 1 V display different shapes compared to traditional capacitive ion storage, which  
 315 seems quite incomprehensible. The curves look almost symmetrical indicating the charge storing  
 316 ability of this composites. Excellent cycling stability of the electrode was obtained, which could be  
 317 due to the unique structural features of the composites. Nafion® could act as a barrier and keep the  
 318 lignin intact within the electrode, which could avoid the loss of active mass in the electrolyte and due  
 319 to its ionic conductivity it could facilitate the charge transfer process by easing the efficient electron  
 320 transport pathway. Additionally, the porous PEO polymer could work as a buffer, which provide the  
 321 strain relaxation and volume change enabling the easy access of the electrolyte passage. Due to  
 322 incomprehension and to be certain EIS measurements were conducted before and after the GCPL  
 323 cycling measurements.



324  
325 **Schematic. 2: Series equivalent electric circuit model created on the basis of structural impedance**  
326 **behaviour of lignin based composite membranes.**

327 Experimental impedance results are represented using Nyquist curves, where a non-linear  
328 adjustment techniques CNLS (complex nonlinear least square) was applied to a series equivalent  
329 circuit model (Schematic. 2). ECM series shows different components, where R1 represents the  
330 resistance of the assembly formed by electrolyte, working electrode and reference electrode. R2 is the  
331 interface resistance related to encapsulation of lignin within PEO and Nafion® structure. In order to  
332 represent the hydrophobic and heterogeneous structure of lignin mixture, CPE1 (constant phase  
333 element) have been used. CPE elements are able to reproduce the inhomogeneity related to the  
334 porous structure of the electrode, mass transfer phenomena or charge transfer reactions. The  
335 characteristics of the double layer are associated to the values of R3 (charge transfer resistance) and  
336 CPE2 (constant phase element).[54–56] Two capacitive arcs have been obtained, whose characteristic  
337 time constants correspond to two CPE-R pairs. The high frequency time constant, associated with the  
338 pair R2/CPE1 reflects the characteristics of the pore resistance and the low-frequency constant,  
339 reflects the characteristics of the load transfer resistance, associated with the pair R3/CPE2. The  
340 experimental impedance values fitted well with the series ECM.

341 To understand the physico-chemical processes within different time constants in the EIS spectra  
342 (Figure 9), the distribution of the relaxation times (DRT) of the experimental impedance data was  
343 calculated.[56–60]. Relaxation times obtained when fitting the impedance data to the ECM model,  
344 with respect to the times obtained when representing the same impedance data through the  
345 polarization processes, and (DRT). From the values of the different CPE1 and CPE2 the values of the  
346 capacitances can be obtained[61,62] as shown in Table S2 and S5.



347 **Figure. 9: Nyquist and DRT plots corresponding to the Impedance spectra of the; a-b) OLPONF**  
348 **and c-d) KLPONF, e-f) OLNf electrodes before and after the GCPL cycling measurements,**  
349 **respectively.**

350 When comparing the time constants ( $\tau$ ) obtained through experimental and DRT calculations, it can  
351 be seen that the obtained results differs, the DRT values have been shown in Table S3. After cycling,  
352 KLPONF shows only a low frequency relaxation time, the high frequency time constant is absent  
353 within the DRT representation. The behavior of all lignin samples follows a decreasing pattern in the  
354 evolution of impedance. In the OLPONF and KLPONF samples this impedance drop is much more  
355 accentuated, decreasing much the interface resistance related to the encapsulation of lignin within  
356 the structure of PEO and Nafion®. The sample that best maintains its initial and final values and  
357 characteristics in a chemical environment is OLNf, possibly due to their structural integrity as shown  
358 by WU and SR% tests results. To validate the EIS data, the statistical analysis of repeated samples  
359 have been calculated (Figure S3), which reflects that the compound are highly electrochemically  
360 responsive depending on their composite mixture, surprisingly the KLPONF and OLPONF  
361 composites have shown more or less similar behavior in SD as well as in variance, however, the OLNf  
362 have been proven to show the highest distributive values.), which could be due to the behavioural  
363 changes of the biomass polymer (lignin) within the polymeric matrix i.e. difference between their  
364 intercross linkages, however, these outcomes need much strict understandings.

### 365 3.6 Perspectives and Limitations:

366 The main goal of this study is to develop lignin-based conductive composite materials and study  
367 their electrochemical properties for applications within electrochemical energy storage (EES) systems  
368 such as battery, fuel cell or supercapacitors. This study validates the idea of activation of lignin redox  
369 properties via simple modification in the polymeric matrix. However, lignin possesses diverse  
370 functionalities and its richness in aromaticity is yet to be explored, thus, our major goal is to provide  
371 a fully organic biomass conductive polymeric matrix via playing and tuning the functional groups of  
372 lignin using only simple and low-cost techniques that could open a door towards economical energy  
373 storage systems. Although, this study proposes an easy and inexpensive casting method to prepare  
374 composite membranes, however, the thickness control is the major limitations of this methodology  
375 that could lead to the probability of error despite following the exact steps and procedure. Thus,  
376 further studies will also be focused on the membrane casting optimization to establish internal and  
377 external validity of the result of unanticipated challenges that could emerged during the study.

## 378 5. Conclusions

379 Stable and functional lignin based composite (OL/KL-PONF) membranes were prepared by an easy  
380 mixing and solution casting method to be used as cheap electrodes. The present work shows  
381 consecutive characterization of the membranes to conclude the improved conductivity, the structural  
382 functionality and integrity. A strong ionic acid in mild reaction conditions was added to facilitate the  
383 pathway of oxidation and activation of the quinone reversible ( $2e^-/2H^+$ ) redox cycling. The FTIR  
384 spectroscopy confirms the formation of composite mixture, where the shift in the vibration band of  
385 C-O-C and C=O stretching and appearance of Si-OH, Si-O-Si and CF<sub>2</sub> was observed due to  
386 incorporation of nafion®. Whereas, electrochemical processes and CV scans confirms the redox  
387 couple behavior and stability over repetitive cycling of the composite membranes. Further studies  
388 will continue on the in-depth understanding of lignin functionalities behavior along with exploration  
389 of potential modification routes and as Nafion® is an expensive polymer, the alternatives are needed  
390 to be studied in order to advance in the optimization of the composite membranes as well as of the  
391 electrochemical process.

392 **Author Contributions:** For research articles with several authors, a short paragraph specifying their  
393 individual contributions must be provided.

394 Marya Baloch has taken part in conceptualization, methodology, validation, formal analysis,  
395 investigation, data curation, writing—original draft preparation, writing—review and editing, and  
396 visualization.

397 Mikel Alberro Astarbe has taken part in formal analysis, data curation, writing—review and editing,  
398 and visualization.

399 Jalel Labidi has taken part in conceptualization, resources, writing—review and editing,  
400 visualization, supervision, project administration, and funding acquisition.

401 **Funding:** This research was funded by the Basque Government (project IT1008-16).

402 **Acknowledgments:** The authors thanks “Florencio Fernandez Marzo” and the laboratory of  
403 Chemical Engineering II at the department of Chemical and Environmental Engineering, School of  
404 Engineering of Gipuzkoa for their help and assistances with the electrochemical equipment.

405 **Conflicts of Interest:**

406 The authors declare no conflict of interest.

407

408 **References**

- 409 1. Chen, H.; Cong, T.N.; Yang, W.; Tan, C.; Li, Y.; Ding, Y. Progress in electrical energy storage  
410 system: A critical review. *Prog. Nat. Sci.* **2009**, *19*, 291–312, doi:10.1016/j.pnsc.2008.07.014.
- 411 2. Tong, Y.; Liang, J.; Liu, H.K.; Dou, S.X. Energy storage in Oceania. *Energy Storage Mater.* **2019**,  
412 doi:10.1016/j.ensm.2019.04.031.
- 413 3. Palomares, V.; Serras, P.; Villaluenga, I.; Hueso, K.B.; Carretero-González, J.; Rojo, T. Na-ion  
414 batteries, recent advances and present challenges to become low cost energy storage systems.  
415 *Energy Environ. Sci.* **2012**, *5*, 5884–5901, doi:10.1039/c2ee02781j.
- 416 4. Zhong, C.; Deng, Y.; Hu, W.; Qiao, J.; Zhang, L.; Zhang, J. A review of electrolyte materials  
417 and compositions for electrochemical supercapacitors. *Chem. Soc. Rev.* **2015**, *44*, 7484–7539,  
418 doi:10.1039/c5cs00303b.
- 419 5. Simon, P.; Gogotsi, Y. Materials for electrochemical capacitors. *Nat. Mater.* **2008**, *7*, 845–854.
- 420 6. Dehghani-Sani, A.R.; Tharumalingam, E.; Dusseault, M.B.; Fraser, R. Study of energy storage  
421 systems and environmental challenges of batteries. *Renew. Sustain. Energy Rev.* **2019**, *104*, 192–  
422 208, doi:10.1016/j.rser.2019.01.023.
- 423 7. Ni, D.; Song, H.; Chen, Y.; Cai, K. Free-standing highly conducting PEDOT films for flexible  
424 thermoelectric generator. *Energy* **2019**, *170*, 53–61, doi:10.1016/j.energy.2018.12.124.
- 425 8. Popov, A.; Brasiunas, B.; Mikoliunaite, L.; Bagdziunas, G.; Ramanavicius, A.; Ramanaviciene,  
426 A. Comparative study of polyaniline (PANI), poly(3,4-ethylenedioxythiophene) (PEDOT) and  
427 PANI-PEDOT films electrochemically deposited on transparent indium thin oxide based  
428 electrodes. *Polymer (Guildf)*. **2019**, *172*, 133–141, doi:10.1016/j.polymer.2019.03.059.
- 429 9. Chen, Q.; Wang, X.; Chen, F.; Zhang, N.; Ma, M. Extremely strong and tough polythiophene  
430 composite for flexible electronics. *Chem. Eng. J.* **2019**, *368*, 933–940,  
431 doi:10.1016/j.cej.2019.02.203.
- 432 10. Dong, J.; Lin, Y.; Zong, H.; Yang, H. Hierarchical LiFe 5 O 8 @PPy core-shell nanocomposites  
433 as electrode materials for supercapacitors. *Appl. Surf. Sci.* **2019**, *470*, 1043–1052,  
434 doi:10.1016/j.apsusc.2018.11.204.
- 435 11. Muniz, C.R.; Cunha, M.S. Effects of strong electric fields in a polyacetylene chain. *J. Phys.*  
436 *Chem. Solids* **2015**, *82*, 17–20, doi:10.1016/j.jpcs.2015.02.009.
- 437 12. Chen, Q.; Yin, Q.; Dong, A.; Gao, Y.; Qian, Y.; Wang, D.; Dong, M.; Shao, Q.; Liu, H.; Han,  
438 B.H.; et al. Metal complex hybrid composites based on fullerene-bearing porous polycarbazole  
439 for H<sub>2</sub>, CO<sub>2</sub> and CH<sub>4</sub> uptake and heterogeneous hydrogenation catalysis. *Polymer (Guildf)*.  
440 **2019**, *169*, 255–262, doi:10.1016/j.polymer.2019.02.056.
- 441 13. Gao, C.; Chen, G. Conducting polymer/carbon particle thermoelectric composites: Emerging

- 442 green energy materials. *Compos. Sci. Technol.* **2016**, *124*, 52–70,  
443 doi:10.1016/j.compscitech.2016.01.014.
- 444 14. Bae, J.; Park, J.Y.; Kwon, O.S.; Lee, C.S. Energy efficient capacitors based on  
445 graphene/conducting polymer hybrids. *J. Ind. Eng. Chem.* **2017**, *51*, 1–11,  
446 doi:10.1016/j.jiec.2017.02.023.
- 447 15. Zhu, H.; Luo, W.; Ciesielski, P.N.; Fang, Z.; Zhu, J.Y.; Henriksson, G.; Himmel, M.E.; Hu, L.  
448 Wood-Derived Materials for Green Electronics, Biological Devices, and Energy Applications.  
449 *Chem. Rev.* **2016**, *116*, 9305–9374, doi:10.1021/acs.chemrev.6b00225.
- 450 16. Silva, F.T.M.; Ataíde, C.H. Valorization of eucalyptus urograndis wood via carbonization:  
451 Product yields and characterization. *Energy* **2019**, *172*, 509–516,  
452 doi:10.1016/j.energy.2019.01.159.
- 453 17. Constant, S.; Wienk, H.L.J.; Frissen, A.E.; Peinder, P. De; Boelens, R.; Van Es, D.S.; Grisel,  
454 R.J.H.; Weckhuysen, B.M.; Huijgen, W.J.J.; Gosselink, R.J.A.; et al. New insights into the  
455 structure and composition of technical lignins: A comparative characterisation study. *Green*  
456 *Chem.* **2016**, *18*, 2651–2665, doi:10.1039/c5gc03043a.
- 457 18. Hirai, N.; Tanaka, T.; Kubo, S.; Ikeda, T.; Magara, K.; Ban, I.; Shiota, M. Density and hardness  
458 of negative pastes of lead-acid batteries containing organic additives with or without quinone  
459 structure. *J. Power Sources* **2006**, *158*, 1106–1109, doi:10.1016/j.jpowsour.2006.02.002.
- 460 19. Jablonsky, M.; Andrea, S.; Haz, A.; Ludmila, H.; Michal, J.; Andrea, Š.; Aleš, H. *Lignin, potential*  
461 *products and their market value*;
- 462 20. Amezcua-Allieri, M.A.; Aburto, J. Conversion of Lignin to Heat and Power, Chemicals or  
463 Fuels into the Transition Energy Strategy. *Lignin - Trends Appl.* **2018**,  
464 doi:10.5772/intechopen.71211.
- 465 21. Xia, K.; Ouyang, Q.; Chen, Y.; Wang, X.; Qian, X.; Wang, L. Preparation and Characterization  
466 of Lignosulfonate-Acrylonitrile Copolymer as a Novel Carbon Fiber Precursor. *ACS Sustain.*  
467 *Chem. Eng.* **2016**, *4*, 159–168, doi:10.1021/acssuschemeng.5b01442.
- 468 22. Lu, H.; Zhao, X.S. Biomass-derived carbon electrode materials for supercapacitors. *Sustain.*  
469 *Energy Fuels* **2017**, *1*, 1265–1281, doi:10.1039/C7SE00099E.
- 470 23. Fang, Z.; Fan, L.; Grace, J.R.; Ni, Y.; Scott, N.R.; Smith, R.L. *Biofuels and Biorefineries*. **6**.
- 471 24. Tenhaeff, W.E.; Rios, O.; More, K.; McGuire, M.A. Highly robust lithium ion battery anodes  
472 from lignin: An abundant, renewable, and low-cost material. *Adv. Funct. Mater.* **2014**, *24*, 86–  
473 94, doi:10.1002/adfm.201301420.
- 474 25. Lu, H.; Cornell, A.; Alvarado, F.; Behm, M.; Leijonmarck, S.; Li, J.; Tomani, P.; Lindbergh, G.  
475 Lignin as a binder material for eco-friendly Li-ion batteries. *Materials (Basel)*. **2016**, *9*, 1–17,  
476 doi:10.3390/ma9030127.



- 477 26. Nirmale, T.C.; Kale, B.B.; Varma, A.J. A review on cellulose and lignin based binders and  
478 electrodes: Small steps towards a sustainable lithium ion battery. *Int. J. Biol. Macromol.* **2017**,  
479 *103*, 1032–1043, doi:10.1016/j.ijbiomac.2017.05.155.
- 480 27. Mukhopadhyay, A.; Hamel, J.; Katahira, R.; Zhu, H. Metal-Free Aqueous Flow Battery with  
481 Novel Ultrafiltered Lignin as Electrolyte. *ACS Sustain. Chem. Eng.* **2018**, *6*, 5394–5400,  
482 doi:10.1021/acssuschemeng.8b00221.
- 483 28. Hill, C.A.S. The Use of Timber in the Twenty-first Century. *Wood Modif.* **2006**, 1–18,  
484 doi:10.1002/0470021748.ch1.
- 485 29. Matrakova, M.; Rogachev, T.; Pavlov, D.; Myrvold, B.O. Influence of phenolic group content  
486 in lignin expanders on the performance of negative lead-acid battery plates. *J. Power Sources*  
487 **2003**, *113*, 345–354, doi:10.1016/S0378-7753(02)00547-5.
- 488 30. Gnedenkov, S. V.; Opra, D.P.; Zemnukhova, L.A.; Sinebryukhov, S.L.; Kedrinskii, I.A.;  
489 Patrusheva, O. V.; Sergienko, V.I. Electrochemical performance of Klason lignin as a low-cost  
490 cathode-active material for primary lithium battery. *J. Energy Chem.* **2015**, *24*, 346–352,  
491 doi:10.1016/S2095-4956(15)60321-7.
- 492 31. Wu, X.; Jiang, J.; Wang, C.; Liu, J.; Pu, Y.; Ragauskas, A.; Li, S.; Yang, B. Lignin-derived  
493 electrochemical energy materials and systems. *Biofuels, Bioprod. Biorefining* **2020**, *14*, 650–672,  
494 doi:10.1002/bbb.2083.
- 495 32. Liu, B.; Huang, Y.; Cao, H.; Song, A.; Lin, Y.; Wang, M.; Li, X. A high-performance and  
496 environment-friendly gel polymer electrolyte for lithium ion battery based on composited  
497 lignin membrane. *J. Solid State Electrochem.* **2018**, *22*, 807–816, doi:10.1007/s10008-017-3814-x.
- 498 33. Chaleawlerumpon, S.; Berthold, T.; Wang, X.; Antonietti, M.; Liedel, C. Kraft Lignin as  
499 Electrode Material for Sustainable Electrochemical Energy Storage. *Adv. Mater. Interfaces* **2017**,  
500 *4*, 1–7, doi:10.1002/admi.201700698.
- 501 34. Casado, N.; Hilder, M.; Pozo-Gonzalo, C.; Forsyth, M.; Mecerreyes, D. Electrochemical  
502 Behavior of PEDOT/Lignin in Ionic Liquid Electrolytes: Suitable Cathode/Electrolyte System  
503 for Sodium Batteries. *ChemSusChem* **2017**, *10*, 1783–1791, doi:10.1002/cssc.201700012.
- 504 35. Wang, S.; Zhang, L.L.; Wang, A.; Liu, X.; Chen, J.; Wang, Z.; Zeng, Q.; Zhou, H.H.; Jiang, X.;  
505 Zhang, L.L. Polymer-Laden Composite Lignin-Based Electrolyte Membrane for High-  
506 Performance Lithium Batteries. *ACS Sustain. Chem. Eng.* **2018**, *6*, 14460–14469,  
507 doi:10.1021/acssuschemeng.8b03117.
- 508 36. Gnedenkov, S.V.V. V; Sinebryukhov, S.L.L.L.; Opra, D.P.P.P.; Zemnukhova, L.A.A.A.;  
509 Tsvetnikov, A.K.K.; Minaev, A.N.N.; Sokolov, A.A.A.; Sergienko, V.I.I. Electrochemistry of  
510 Klason Lignin. *Procedia Chem.* **2014**, *11*, 96–100, doi:10.1016/j.proche.2014.11.018.
- 511 37. Gnedenkov, S. V.; Opra, D.P.; Sinebryukhov, S.L.; Tsvetnikov, A.K.; Ustinov, A.Y.; Sergienko,

- 512 V.I. Hydrolysis lignin: Electrochemical properties of the organic cathode material for primary  
513 lithium battery. *J. Ind. Eng. Chem.* **2014**, *20*, 903–910, doi:10.1016/j.jiec.2013.06.021.
- 514 38. Ye, J.; Lou, X.; Wu, C.; Wu, S.; Ding, M.; Sun, L.; Jia, C.; Ding, M. Ion Selectivity and Stability  
515 Enhancement of SPEEK / Lignin Membrane for Vanadium Redox Flow Battery : The Degree  
516 of Sulfonation Effect. *Front. Chem.* **2019**, *6*, 1–9, doi:10.3389/fchem.2018.00549.
- 517 39. Ye, J.; Cheng, Y.; Sun, L.; Ding, M.; Wu, C.; Yuan, D.; Zhao, X.; Xiang, C.; Jia, C. A green  
518 SPEEK/lignin composite membrane with high ion selectivity for vanadium redox flow  
519 battery. *J. Memb. Sci.* **2019**, *572*, 110–118, doi:10.1016/j.memsci.2018.11.009.
- 520 40. Admassie, S.; Ajan, F.N.; Elfwing, A.; Inganäs, O. Biopolymer hybrid electrodes for scalable  
521 electricity storage. *Mater. Horizons* **2016**, *3*, 174–185, doi:10.1039/c5mh00261c.
- 522 41. Rębiś, T.; Nilsson, T.Y.; Inganäs, O. Hybrid materials from organic electronic conductors and  
523 synthetic-lignin models for charge storage applications. *J. Mater. Chem. A* **2016**, *4*, 1931–1940,  
524 doi:10.1039/c5ta06821e.
- 525 42. Milczarek, G. Lignosulfonate-modified electrodes: Electrochemical properties and  
526 electrocatalysis of NADH oxidation. *Langmuir* **2009**, *25*, 10345–10353, doi:10.1021/la9008575.
- 527 43. Milczarek, G. Preparation and characterization of a lignin modified electrode. *Electroanalysis*  
528 **2007**, *19*, 1411–1414, doi:10.1002/elan.200703870.
- 529 44. Lota, G.; Milczarek, G. The effect of lignosulfonates as electrolyte additives on the  
530 electrochemical performance of supercapacitors. *Electrochem. commun.* **2011**, *13*, 470–473,  
531 doi:10.1016/j.elecom.2011.02.023.
- 532 45. Zhu, J.; Yan, C.; Zhang, X.; Yang, C.; Jiang, M.; Zhang, X. A sustainable platform of lignin:  
533 From bioresources to materials and their applications in rechargeable batteries and  
534 supercapacitors. *Prog. Energy Combust. Sci.* **2020**, *76*, 100788, doi:10.1016/j.pecs.2019.100788.
- 535 46. Becker, J.; Wittmann, C. A field of dreams: Lignin valorization into chemicals, materials, fuels,  
536 and health-care products. *Biotechnol. Adv.* **2019**, *37*, 107360,  
537 doi:10.1016/j.biotechadv.2019.02.016.
- 538 47. Editors: Hakeem, Khalid Rehman, Jawaid, Mohammad, Alothman, O. *Agricultural Biomass*  
539 *Based Potential Materials*; 2015; ISBN 9783319138473.
- 540 48. Obydenkova, S. V.; Kouris, P.D.; Hensen, E.J.M.M.; Heeres, H.J.; Boot, M.D. Environmental  
541 economics of lignin derived transport fuels. *Bioresour. Technol.* **2017**, *243*, 589–599,  
542 doi:10.1016/j.biortech.2017.06.157.
- 543 49. Ragauskas, A.J.; Beckham, G.T.; Bidy, M.J.; Chandra, R.; Chen, F.; Davis, M.F.; Davison, B.H.;  
544 Dixon, R.A.; Gilna, P.; Keller, M.; et al. Lignin valorization: Improving lignin processing in the  
545 biorefinery. *Science (80-. )*. **2014**, *344*, doi:10.1126/science.1246843.

- 546 50. Ding, R.; Wu, H.; Thunga, M.; Bowler, N.; Kessler, M.R. Processing and characterization of  
547 low-cost electrospun carbon fibers from organosolv lignin/polyacrylonitrile blends. *Carbon N.*  
548 *Y.* **2016**, *100*, 126–136, doi:10.1016/j.carbon.2015.12.078.
- 549 51. Fodil Cherif, M.; Trache, D.; Brosse, N.; Benaliouche, F.; Tarchoun, A.F. Comparison of the  
550 Physicochemical Properties and Thermal Stability of Organosolv and Kraft Lignins from  
551 Hardwood and Softwood Biomass for Their Potential Valorization. *Waste and Biomass*  
552 *Valorization* **2020**, *11*, 6541–6553, doi:10.1007/s12649-020-00955-0.
- 553 52. Liu, G.; Shi, H.; Ping, Q.; Zhou, J.; Zhang, J.; Li, N.; Niu, M.; Fatehi, P.; Xiao, H.; Ni, Y. Complex  
554 Formation of PEO and Lignin in Prehydrolysis Liquor and its Enhancing Effect on Lignin  
555 Removal. *BioResources* **2013**, *8*, 4004–4015, doi:10.15376/biores.8.3.4004-4015.
- 556 53. Kubo, S.; Kadla, J.F. Kraft lignin/poly(ethylene oxide) blends: Effect of lignin structure on  
557 miscibility and hydrogen bonding. *J. Appl. Polym. Sci.* **2005**, *98*, 1437–1444,  
558 doi:10.1002/app.22245.
- 559 54. Chen, T.; Zhang, Q.; Xu, J.; Pan, J.; Cheng, Y.T. Binder-free lithium ion battery electrodes made  
560 of silicon and pyrolyzed lignin†. *RSC Adv.* **2016**, *6*, 29308–29313, doi:10.1039/c6ra03001g.
- 561 55. Stergiou, D. V.; Veltsistas, P.G.; Prodromidis, M.I. An electrochemical study of lignin films  
562 degradation: Proof-of-concept for an impedimetric ozone sensor. *Sensors Actuators, B Chem.*  
563 **2008**, *129*, 903–908, doi:10.1016/j.snb.2007.10.001.
- 564 56. Illig, J.; Chrobak, T.; Klotz, D.; Ivers-Tiffée, E. Evaluation of the Rate Determining Processes  
565 for LiFePO<sub>4</sub> as Cathode Material in Lithium-Ion-Batteries. *ECS Trans.* **2019**, *33*, 3–15,  
566 doi:10.1149/1.3564865.
- 567 57. <https://sites.google.com/site/drttools/>.
- 568 58. Ciucci, F.; Chen, C. Analysis of electrochemical impedance spectroscopy data using the  
569 distribution of relaxation times: A Bayesian and hierarchical Bayesian approach. *Electrochim.*  
570 *Acta* **2015**, *167*, 439–454, doi:10.1016/j.electacta.2015.03.123.
- 571 59. Schmidt, J.P.; Chrobak, T.; Ender, M.; Illig, J.; Klotz, D.; Ivers-Tiffée, E. Studies on LiFePO<sub>4</sub> as  
572 cathode material using impedance spectroscopy. *J. Power Sources* **2011**, *196*, 5342–5348,  
573 doi:10.1016/j.jpowsour.2010.09.121.
- 574 60. Li, X.; Ahmadi, M.; Collins, L.; Kalinin, S. V. Deconvolving distribution of relaxation times,  
575 resistances and inductance from electrochemical impedance spectroscopy via statistical model  
576 selection: Exploiting structural-sparsity regularization and data-driven parameter tuning.  
577 *Electrochim. Acta* **2019**, *313*, 570–583, doi:10.1016/j.electacta.2019.05.010.
- 578 61. Li, Q.; Thangadurai, V. Synthesis, Structure and Electrical Properties of Mo-doped CeO<sub>2</sub>-  
579 Materials for SOFCs. *Fuel Cells* **2009**, *9*, 684–698, doi:https://doi.org/10.1002/fuce.200900044.
- 580 62. Li, Q.; Xia, T.; Liu, X.D.; Ma, X.F.; Meng, J.; Cao, X.Q. Fast densification and electrical

581 conductivity of yttria-stabilized zirconia nanoceramics. *Mater. Sci. Eng. B Solid-State Mater.*  
582 *Adv. Technol.* **2007**, *138*, 78–83, doi:10.1016/j.mseb.2006.12.012.

583 **Publisher’s Note:** MDPI stays neutral with regard to jurisdictional claims in published maps and  
584 institutional affiliations.



© 2020 by the authors. Submitted for possible open access publication under the terms and conditions of the Creative Commons Attribution (CC BY) license (<http://creativecommons.org/licenses/by/4.0/>).

585